Scientific report for the project Idei nr 160/2021

Period: January-December 2021

In the period January-December 2021 the scientific activity was concentrated to the following subjects, specified in the program for the current year: (A) Extension of the QCM approach for the description of excited states of systems with N=Z nucleons interacting by: (a1) proton-neutron pairing interactions and (a2) general two-body interactions of shell model type; (B) Contribution of isovector and isoscalar proton-neutron pairing correlations to the ground and excited states of self-conjugate nuclei.

Related to these subjects, we have performed the following studies:

I) We have proposed a new QCM formalism for calculating the excited states of proton-neutron pairing Hamiltonians. We have shown that these states can be described by breaking a quartet from the ground state condensate and replacing it with an "excited" quartet. This approach, which is analogous to the one-broken-pair approximation employed for like-particle pairing, was analysed for various isovector and isovector-isoscalar pairing Hamiltonians which can be solved exactly by diagonalisation.

II) We have extended the quartet model to treat the excited states of N=Z nuclei in which the valence nucleons are interacting by a realistic two-boy force of shell model type. The excited states are constructed in terms of quartets which are extracted from various intrinsic states. The new formalism was applied to the N=Z nuclei ^{24}Mg, ^{28}Si and ^{48}Cr and it was studied, for these nuclei, the contribution of various quartets to the ground and excited states energies. In particular, it was shown that the new quartet formalism allows to identify band-like structures in the low-lying states of these nuclei.

III) We have investigated, in a Skyrme+QCM formalism, the contribution of proton-neutron pairing correlations to the binding energies of nuclei close to N=Z line. The novel feature of the present calculations is that they take into account dynamically the competition between pairing and deformation in a formalism which conserves exactly both the particle number and the isospin. We have shown that the main contribution to the binding energies comes from the isovector proton-neutron pairing correlations.

The results of these studied have been presented in the following articles:

- α-like quartetting in the excited states of proton-neutron pairing Hamiltonians [1]

- Band-like structures and quartets in deformed $N = Z$ nuclei [2]
- Proton-neutron pairing and binding energies of nuclei close to N=Z line [3]

Below we present the shorter versions of these article, which describe in detail the studied mentioned above.

I. α-LIKE QUARTETTING IN THE EXCITED STATES OF PROTON-NEUTRON PAIRING HAMILTONIANS [1]

Previous studies have shown that the ground state of systems of nucleons composed by an equal number of protons and neutrons interacting via proton-neutron pairing forces can be described accurately by the Quartet Condensation Model (QCM) [4–7] in which the ground state of these systems is approximated by a condensate of α-like quartets. Here we extend the QCM approach to the excited states of N=Z systems interacting by an isovector (T=1) and an isoscalar (T=0) pairing force.

A. Excited states for the isovector pairing

The isovector pairing Hamiltonian has the expression

$$H = \sum_i \epsilon_i N_i + \sum_{i,j} V_{J=0}^{T=1}(i,j) \sum_{T_z} P_{i,T_z}^{+} P_{j,T_z}^{+} \tag{1}$$

where

$$N_i = \sum_{\sigma=\pm,\tau=\pm\frac{1}{2}} a_{i\sigma\tau}^{\dagger} a_{i\sigma\tau}, \qquad P_{i,T_z}^{+} = \sqrt{\frac{2j_i+1}{2}} [a_i^{+} a_i^{+}]_{T_z}^{T=1,J=0}. \tag{2}$$

The operator $a_{i\sigma\tau}^{\dagger}$ ($a_{i\sigma\tau}$) creates (annihilates) a nucleon in the single-particle state i characterized by the quantum numbers (σ, τ), where $\sigma = \pm$ labels states which are conjugate with respect to time reversal and $\tau = \pm\frac{1}{2}$ is the projection of the isospin of the nucleon. The operator $P_{iT_z}^{\dagger}$ (P_{iT_z}) creates (annihilates) a pair of nucleons in time-reversed states with total isospin $T = 1$. The three isospin projection T_z correspond to pp, nn and pn pairs. In Eq.(2) the pair operators are written for the case of a spherically-symmetric Hamiltonian with pairs which have a well-defined angular momentum J=0.

We start by recalling the quartet condensation model (QCM) for the ground state of this Hamiltonian, which will be used below for introducing the new class of excited states. In Ref. [6] it was shown that the ground state of the Hamiltonian (1) with $n_q/2$ active protons and neutrons can be well approximated by a quartet condensate:

$$|QCM\rangle = (Q_{iv}^{+})^{n_q}|-\rangle \tag{3}$$

where

$$Q_{iv}^{+} = \sum_{ij} x_{ij}[P_i^{\dagger}P_j^{\dagger}]^{T=0} = \sum_{ij} x_{ij}\frac{1}{\sqrt{3}}(P_{i1}^{\dagger}P_{j-1}^{\dagger} + P_{i-1}^{\dagger}P_{j1}^{\dagger} - P_{i0}^{\dagger}P_{j0}^{\dagger}) \tag{4}$$

is the collective quartet built by a linear combination of two non-collective isovector pairs coupled to the total isospin $T = 0$. By construction the quartet (4) contains two types of 4-body correlations between the protons and neutrons: (a), those generated by the isospin coupling and, (b), those arising from the the mixing parameters x_{ij}.

In order to study the excitation spectrum of the Hamiltonian (1) for the same system of protons and neutrons, we consider a new class of QCM states obtained by removing a quartet from the condensate describing the ground state and replacing it with a new "excited" quartet. The excited states have the form

$$|\Phi_\nu\rangle = \tilde{Q}_\nu^{+}(Q_{iv}^{+})^{n_q-1}|-\rangle, \tag{5}$$

where

$$\tilde{Q}_\nu^{+} = \sum_{ij} y_{ij}^{(\nu)}[P_i^{+}P_j^{+}]^{T=0} \tag{6}$$

represents the excited collective quartet. These excited states are therefore linear superpositions of the states

$$[P_i^{+}P_j^{+}]^{T=0}(Q_{iv}^{+})^{n_q-1}|-\rangle. \tag{7}$$

In order to construct the amplitudes $y_{ij}^{(\nu)}$ defining the collective quartet $\tilde{Q}_\nu^{+}$ it suffices to diagonalize the Hamiltonian (1) in the space spanned by the non-orthogonal states (7).

To test this approximation, we shall consider a system with 6 protons and 6 neutrons interacting trough a state independent isovector pairing force (i.e. $V_{J=0}^{T=1}(i,j) \equiv -g$ in Eq. (1)) and distributed over 6 equidistant levels with four-fold degeneracy (due to the presence of both spin and isospin degrees of freedom).

In Fig. 1a we compare the excitation energies corresponding to the ansatz (5), called the approximation (A), as a function of the pairing strength g, with the exact results obtained

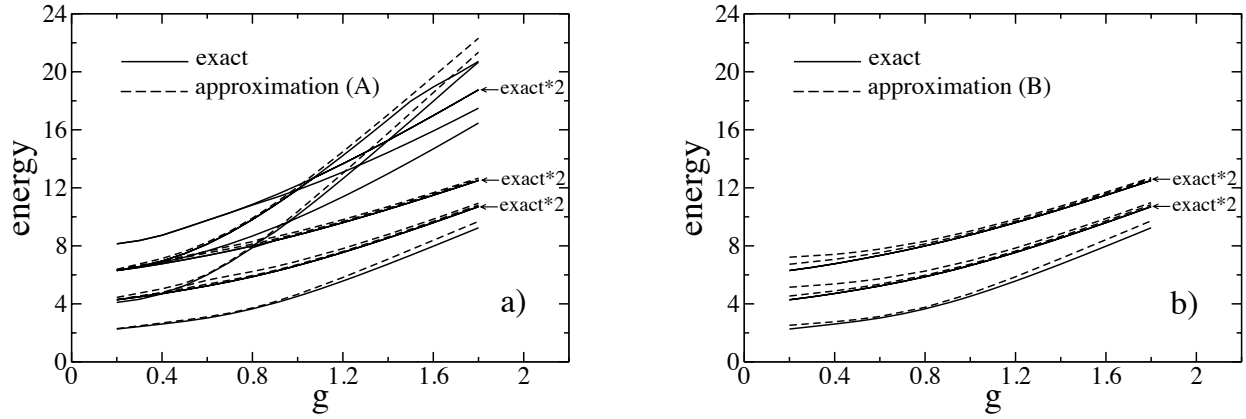

FIG. 1: Excitation spectra of the isovector pairing Hamiltonian (1) for a system of $N = Z = 6$ particles moving on 6 equidistant levels. Dashed lines in Figs. 1a and 1b refer, respectively, to the approximations (A) and (B) discussed in the text while full lines represent the exact results. Energies and the pairing strength g are in units of the spacing $\Delta\epsilon$ between the levels.

by diagonalisation. One can observe that the approximation (A) works well for all pairing strengths, from weak to strong coupling regimes. It can be also noticed that the exact low-lying spectrum contains a few states which cannot be represented by the approximation (A).

In addition to the states described by Eq. (5), we have also explored a particular class of excited states in which the quartets in Eq. (5) are expressed in terms of collective pairs. These quartets are expresed by

$$\overline{Q}^+_{iv} = 2\Gamma^+_1\Gamma^+_{-1} - (\Gamma^+_0)^2 \tag{8}$$

where $\Gamma^+_t = \sum x_i P^+_{it}$. The results corresponding to this approximation, called approximation (B), are shown in Fig. 1b. It can be seen that this approximation works also very well but it does not include all the excited states of approximation (A).

In order to better understand the quality of the Approximations (A) and (B), in Fig. 2 we show a more detailed description of the results of these approximations in a specific case. The calculations of this figure refer to a value of the strength $g = 1.0$ and report not only the spectra but also the overlaps between exact and approximate eigenstates. One can notice that the overlaps are very large both in the approximation (A) and (B). An overlap

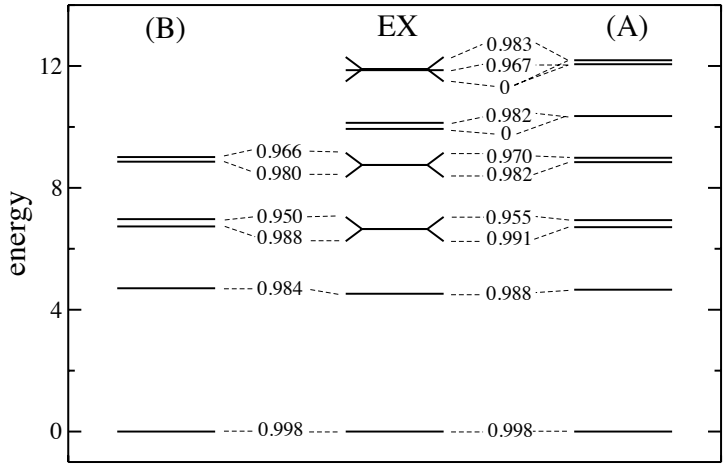

FIG. 2: Low-lying spectra of the isovector pairing Hamiltonian (1) for the same system discussed in Fig. 1 and a pairing strength $g = 1$. The spectra (A) and (B) refer, respectively, to the Approximations (A) and (B) discussed in the text while the spectrum EX corresponds to the exact one. Energies and the pairing strength g are in units of the spacing $\Delta\epsilon$ between the levels.

equal to zero indicates that the corresponding exact eigenstate is not a QCM state.

B. Excited states for the isovector-isoscalar pairing

The isovector-isoscalar pairing Hamiltonian has the expression

$$H = \sum_i \epsilon_i N_i + \sum_{i,j} V^{T=1}_{J=0}(i,j) \sum_{T_z} P^+_{i,T_z} P_{j,T_z} + \sum_{i\leq j,k\leq l} V^{T=0}_{J=1}(ij,kl) \sum_{J_z} D^+_{ij,J_z} D_{kl,J_z}. \quad (9)$$

The first two terms are the same as in Eq. (1) while the last term is the isoscalar pairing interaction written in term of the isoscalar pair operator

$$D^+_{j_1 j_2 J_z} = \frac{1}{\sqrt{1+\delta_{j_1 j_2}}} [a^+_{j_1} a^+_{j_2}]^{J=1,T=0}_{J_z} \quad (10)$$

As in the previous section, we start by recalling the QCM approach for the ground state of the isovector-isoscalar Hamiltonian [7]. For even-even $N = Z$ systems the QCM ansatz for the ground state has formally the same expression as in the case of isovector pairing

$$|\Psi_{gs}\rangle = (Q^+_{ivs})^{n_q} |0\rangle. \quad (11)$$

The difference is that now the quartet operator Q^+_{ivs}, still having total isospin $T = 0$, is the sum of two quartets

$$Q^+_{ivs} = Q^+_{iv} + Q^+_{is}, \tag{12}$$

where Q^+_{iv} is the quartet (6) built by isovector pairs while Q^+_{is} is formed by two isoscalar pairs coupled to total $J = 0$, i.e.,

$$Q^+_{is} = \sum_{j_1 j_2 j_3 j_4} y_{j_1 j_2 j_3 j_4} [D^+_{j_1 j_2} D^+_{j_3 j_4}]^{J=0}. \tag{13}$$

Acting as in the isovector pairing case, in correspondence with the QCM ansatz (11) for the ground state, we construct a class of excited states by replacing a quartet of the condensate with an "excited" quartet. For the case of a spherically-symmetric mean field, these states take the form

$$|\Phi_{\nu,JJ_z}\rangle = \tilde{Q}_{\nu,JJ_z} (Q^+_{ivs})^{n_q-1} |-\rangle, \tag{14}$$

where

$$\tilde{Q}^+_{\nu,JJ_z} = \sum_{T'} \sum_{J_1(i_1 j_1)} \sum_{J_2(i_2 j_2)} Y^{(\nu)}_{JJ_z}(T', J_1(i_1 j_1), J_2(i_2 j_2)) [P^+_{J_1,T'}(i_1, j_1) P^+_{J_2,T'}(i_2, j_2)]^{J,T=0}_{J_z}. \tag{15}$$

In order to determine the coefficients $Y^{(\nu)}_{JJ_z}$ one has to diagonalize the Hamiltonian (9) in the basis of non-orthogonal states

$$[P^+_{J_1,T'}(i_1, j_1) P^+_{J_2,T'}(i_2, j_2)]^{J,T=0}_{J_z} (Q^+_{ivs})^{n_q-1} |-\rangle. \tag{16}$$

To illustrate the accuracy of the approximation (14) we consider a system formed by 6 protons and 6 neutrons above ^{16}O, corresponding to the nucleus ^{28}Si. We assume that these nucleons interact by an isovector-isoscalar pairing force corresponding to the $(J = 0, T = 1)$ and $(J = 1, T = 0)$ channels of the the USDB interaction [8]. Exact and approximate spectra are shown in Fig. 3. The overall agreement is good, although the quality of the overlaps is, in some cases, not as high as in the case of isovector force. As a peculiarity, we notice that the first excited $J = 6$ state has not a corresponding state in the QCM approximation while the second $J = 6$ exact state is well reproduced both for the energy and the overlap.

Summarizing, the low-lying excited states predicted by the extended QCM approach have compared well with the exact eigenstates for both the isovector and the isoscalar-isosvector pairing forces.

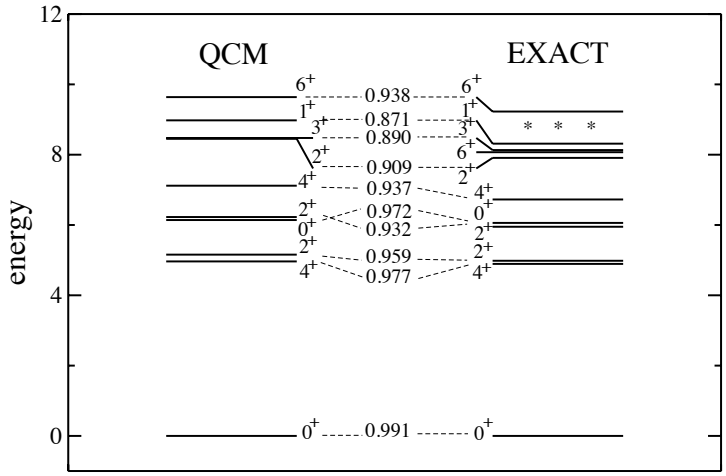

FIG. 3: The low-lying spectrum provided by the QCM approximation (14) for the valence nucleons of ^{28}Si interacting by an isovector-isoscalar pairing force extracted from the USDB interaction. The numbers are the overlaps between the QCM and the exact wave functions. Energies are in MeV.

We like to conclude by noticing the interesting analogy between the eigenstates of proton-neutron and like-particle paring Hamiltonians. As already pointed out in previous studies, the QCM ansatz for the ground state of even-even N=Z systems is the analogous of the particle-number projected-BCS (PBCS) approximation for like-particle systems proposed many years ago by Bayman and Blatt [9, 10]. On the other hand, the one-broken-quartet approximation for the excited states of $N = Z$ systems discussed in the present work shows a clear analogy with the one-broken-pair approximation employed for the treatment the excited states in like-particle systems [11].

II. BAND-LIKE STRUCTURES AND QUARTETS IN DEFORMED $N = Z$ NUCLEI [2]

In this paper the quartet model is extended to treat the excited states of N=Z nuclei in which the valence nucleons are interacting by a general two-boy force of shell model type.The new quartet model is based on dynamical quartets defined in relation to intrinsic

states associated to various bands.

We start by presenting the definition of the quartets and then we introduce, in terms of these quartets, the intrinsic states associated to various bands.

We work in a spherically symmetric mean field and, using the standard notation, we introduce the label $i \equiv \{n_i, l_i, j_i\}$ to identify the orbital quantum numbers. We define the $T = 0$ quartet creation operator as

$$q^+_{JM} = \sum_{i_1 j_1 J_1} \sum_{i_2 j_2 J_2} \sum_{T'} q_{i_1 j_1 J_1, i_2 j_2 J_2, T'} [[a^+_{i_1} a^+_{j_1}]^{J_1 T'} [a^+_{i_2} a^+_{j_2}]^{J_2 T'}]^{JT=0}_M, \tag{17}$$

where a^+_i creates a fermion on the orbital i and M stands for the projection of J. No restrictions on the intermediate couplings $J_1 T'$ and $J_2 T'$ are introduced and the amplitudes $q_{i_1 j_1 J_1, i_2 j_2 J_2, T'}$ are supposed to guarantee the normalization of the operator. We shall focus on systems of N_π protons and N_ν neutrons such that $N_\pi = N_\nu$ and $N_\pi + N_\nu = 4n$ $(n = 2, 3)$ and shall assume axially symmetry. Once quartets have been fixed, we generate the energy spectra by carrying out configuration-interaction calculations.

As a starting point we introduce the state

$$|\Theta_g\rangle = \mathcal{N}_g (Q^+_g)^n |0\rangle, \tag{18}$$

where

$$Q^+_g = \sum_J \alpha_{g,J} (q^+_g)_{J0} \tag{19}$$

and $\mathcal{N}_g$ a normalization factor. $|\Theta_g\rangle$ is thus a condensate of the quartet Q^+_g which is a linear superposition of quartets $(q^+_g)_{J0}$ of the general form (17) and whose angular momentum J runs over a set of values to be specified. After fixing this set of values, we minimize the energy of the state $|\Theta_g\rangle$ and so define the quartets $(q^+_g)_J$ (let's call these "dynamical" quartets). We are then ready to carry out configuration-interaction calculations in a space spanned by these quartets. In Figs. 4,5 and 6, columns (A) and (B), we show what changes occur in the low-lying spectra of the nuclei under study when a set of dynamical quartets replace the analogous set of static quartets associated with the neighboring $T = 0$ systems. In the columns (A) we plot all the positive parity states up to the 6_1 obtained using a set of static J=0,2,4 (plus J=6 in the case of ^{48}Cr) quartets. In spite of the quite good results for the ground state correlation energy (defined as the difference between the ground state energies with and in absence of interaction), in all cases the spectra show marked

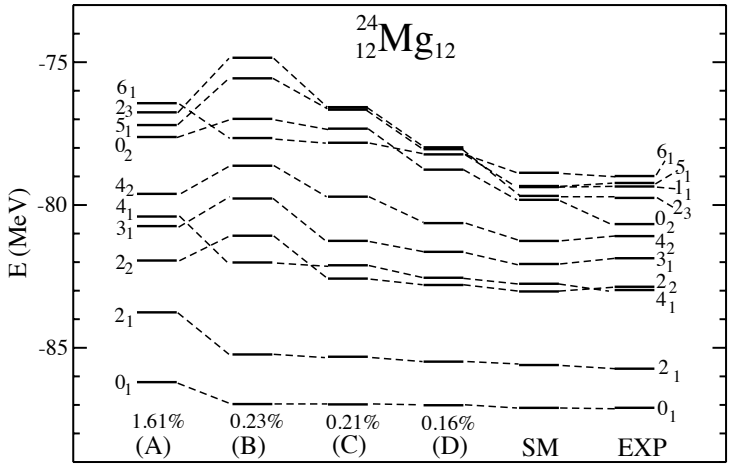

FIG. 4: Spectra of ^{24}Mg obtained by performing configuration-interaction calculations in spaces built with various sets of $T = 0$ quartets (see text): (A), $J = 0, 2, 4$ static quartets from ^{20}Ne; (B), $J = 0, 2, 4$ dynamical quartets from the ground intrinsic state; (C), the same set as in (B) plus $J = 2, 3, 4$ quartets from the γ intrinsic state; (D), the same sets as in (C) plus $J = 0, 2, 4$ quartets from the β intrinsic state; SM, shell model results; EXP, experimental spectrum.

differences with respect to the shell model results. In the columns (B) of the same figures, the dynamical quartets with the same J's as above have been employed. In all three nuclei one observes a lowering of the yrast states $J = 0, 2, 4, 6$ forming the ground state bands while most of the remaining states are pushed up in energy. The new ground state bands are all closer in energy to the shell model ones and a considerable improvement is observed also in the accuracy of the ground state correlation energies. Thus adopting the quartets $(q_g^+)_{J0}$ associated with $|\Theta_g\rangle$ has had a positive effect only on the ground state bands of the nuclei under study. The state (18) will be referred to as "ground" intrinsic state.

The not yet satisfactory agreement between the spectra (B) of Figs. 4,5 and 6 and the corresponding shell model spectra makes clear that new quartets must come into play. To this end, by starting from $|\Theta_g\rangle$ and promoting one of the quartets Q_g^+ to an excited configuration, we generate new intrinsic states. We define a "β" intrinsic state as

$$|\Theta_\beta\rangle = \mathcal{N}_\beta Q_\beta^\dagger (Q_g^\dagger)^{(n-1)}|0\rangle, \tag{20}$$

where

$$Q^\dagger_\beta = \sum_J \alpha_{\beta,J} (q^\dagger_\beta)_{J0} \tag{21}$$

and $(q^\dagger_\beta)_{J0}$ a quartet of the general form (17). Assuming that the quartets $(q^+_g)_{J0}$ have already been fixed, we construct the new quartets $(q^\dagger_\beta)_{J0}$ by minimizing the energy of $|\Theta_\beta\rangle$ under the constraint of orthogonality to $|\Theta_g\rangle$.

Similarly, we define a"γ" intrinsic state as

$$|\Theta_\gamma\rangle = \mathcal{N}_\gamma Q^\dagger_\gamma (Q^\dagger_g)^{(n-1)} |0\rangle, \tag{22}$$

where

$$Q^\dagger_\gamma = \sum_J \alpha_{\gamma,J} (q^\dagger_\gamma)_{J2}. \tag{23}$$

and $(q^\dagger_\gamma)_{J2}$ a quartet still of the general form (17) but characterized by an angular momentum projection $M = 2$. More generally, we define a "k" (k=3,4,...) intrinsic state as

$$|\Theta_k\rangle = \mathcal{N}_k Q^\dagger_k (Q^\dagger_g)^{(n-1)} |0\rangle, \tag{24}$$

with

$$Q^\dagger_k = \sum_J \alpha_{k,J} (q^\dagger_k)_{Jk}. \tag{25}$$

where quartets $(q^\dagger_k)_{Jk}$, still of the general form (17), are characterized by an angular momentum projection $M = k$. In these two last cases the new intrinsic quartets $Q^\dagger_\gamma$ and $Q^\dagger_k$ are constructed variationally without any special constraint.

We proceed by observing, case-by-case, how the use of these new intrinsic states can help to improve the spectra of the nuclei under study. In ^{24}Mg, Fig. 4(B), one notices that a band formed by the $J_k = 2_2, 3_1, 4_2, 5_1$ states has been shifted higher in energy when passing from static to dynamical quartets. By making use of the definition of the γ intrinsic state (22), we have constructed new quartets $(q^\dagger_\gamma)_J$ with $J = 2, 3, 4$ and performed a configuration interaction calculation that includes these new quartets in addition to those already used for the calculation of Fig. 4(B). The new result is shown in Fig. 4(C). We observe a clear lowering of the energies of the states $J_k = 2_2, 3_1, 4_2, 5_1$ while the states of the ground state band have remained basically unmodified with respect to those of column (B). The inclusion of the quartets derived with the help of the γ intrinsic state (22) have therefore essentially affected only those which can be associated to a γ band of ^{24}Mg (and, in addition, the state

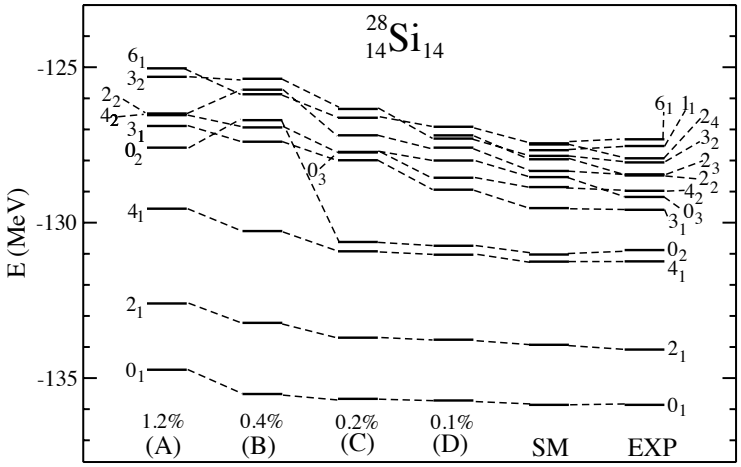

FIG. 5: Spectra of ^{28}Si obtained by performing configuration-interaction calculations in spaces built with various sets of $T = 0$ quartets (see text): (A), $J = 0, 2, 4$ static quartets from ^{20}Ne; (B), $J = 0, 2, 4$ dynamical quartets from the ground intrinsic state; (C), the same set as in (B) plus $J = 0, 2, 4$ quartets from the β intrinsic state; (D), the same sets as in (C) plus $J = 3, 4$ quartets from the $K = 3$ intrinsic state; SM, shell model results; EXP, experimental spectrum.

2_3). As a final step, we have explored the effect on this spectrum of the inclusion of a set of quartets $(q^\dagger_\beta)_J$ with $J = 0, 2, 4$. The basic effect which can be observed in Fig. 4(D) is a lowering the states $J = 0_2, 2_3$ which can be associated to a β band of ^{24}Mg. As a result of the new diagonalization, also the 5_1 state is lowered in energy. The final spectrum shows a good agreement with the shell model one.

For what concerns ^{28}Si, what is most striking in the spectrum of Fig. 5(B) is the absence of a state 0_2 close to the state 4_1 as observed in both the shell model and the experimental spectrum. By interpreting this state 0_2 as the head of a β band, as a next step, we enlarge the model space by also including the quartets $(q^\dagger_\beta)_J$ with $J = 0, 2, 4$ associated with the β intrinsic state. The result of the new configuration calculation can be seen in Fig.5(C). The inclusion of the new quartets mostly affects the yrare $J = 0, 2$ states by giving rise, in particular, to a surprising lowering of the 0_2 state which positions itself immediately above the 4_1 state, where it is expected to be. In spite of the fact that a reasonably

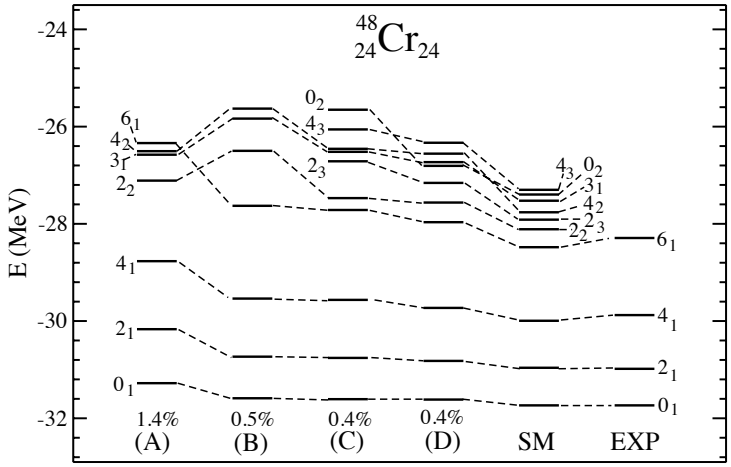

FIG. 6: Spectra of ^{48}Cr obtained by performing configuration-interaction calculations in spaces built with various sets of $T = 0$ quartets (see text): (A), $J = 0, 2, 4, 6$ static quartets from ^{44}Ti; (B), $J = 0, 2, 4, 6$ dynamical quartets from the ground intrinsic state; (C), the same set as in (B) plus $J = 2, 3, 4$ quartets from the γ intrinsic state; (D), the same sets as in (C) plus $J = 0, 2, 4$ quartets from the β intrinsic state; SM, shell model results; EXP, experimental spectrum.

good agreement with the shell model spectrum has already been achieved, we perform an additional calculation which also includes the quartets $(q^\dagger_3)_{J3}$, with $J = 3, 4$, associated with the $k = 3$ intrinsic state (24). Such a new calculation finds its reason for being in an old analysis of ^{28}Si [13] which proposed a classification for bands of its excited states with the band head of a $k = 3$ band positioned immediately above the 0_2 state. As it can be seen in Fig. 5(D), the new calculation essentially lowers the energy of the 3_1 and 4_2 states and, in addition, also that of the 3_2 state. This new calculation further improves the quality of the QM spectrum which compares well with the shell model one.

The last case under investigation, ^{48}Cr, shares some analogies with the corresponding one of ^{24}Mg. Indeed one observes in Fig. 6(B) that, also in this case, the states $2_2, 3_1, 4_2$ have been shifted higher in energy when replacing the static quartets with the corresponding dynamical ones associated with the ground intrinsic state. These states reminding those of a γ band, we proceed as for ^{24}Mg by introducing the quartets $(q^\dagger_\gamma)_J$, associated with the γ

intrinsic state (22), with $J = 2, 3, 4$. The new calculation, Fig. 6(C), leaves unaffected the states of the ground rotational band (as for ^{24}Mg) while it lowers significantly the states $2_2, 3_1, 4_2$. The new calculation also leads to the appearance of new states $(2_3, 4_3, 0_2)$ in the highest part of the spectrum. These states have a correspondence with the shell model ones but with a 0_2 still too high in energy. By interpreting this state as a possible band head of β band and wishing to improve its energy, we perform a final calculation which includes also the quartets $(q^\dagger_\beta)_J$ with $J = 0, 2, 4$. This calculation leads to a significant lowering of the 0_2 state (Fig. 6(D)) which makes the agreement between exact and approximate spectra satisfactory.

Summarizing, in this paper we have provided a description of deformed N = Z nuclei in a formalism of α-like quartets. Quartets have been constructed variationally by resorting to the use of proper intrinsic states while the spectra have been obtained by carrying out configuration-interaction calculations in spaces built with these quartets. The intriguing aspect of these calculations has been the observation of band-like structures associated with the various sets of quartets. As a general conclusion, the present results show that the quartets, defined by the new method proposed in this study, are the proper degrees of freedom for the description of the ground and excited states of deformed N = Z nuclei.

III. PROTON-NEUTRON PAIRING AND BINDING ENERGIES OF NUCLEI CLOSE TO N=Z LINE [3]

To evaluate the contribution of pairing correlations to the binding energies, we employ the QCM approach introduced in Refs [5, 14]. Thus, according to QCM, the ground state for even-even $N = Z$ systems is approximated by the trial state [5]

$$|QCM\rangle = (A^\dagger + \Delta_0^{\dagger 2})^{n_q}|0\rangle, \tag{26}$$

where $n_q = (N + Z)/2$ and $A^\dagger$ is the isovector quartet defined by

$$A^\dagger = 2\Gamma_1^\dagger\Gamma_{-1}^\dagger - (\Gamma_0^\dagger)^2, \tag{27}$$

The operators $\Gamma_t^\dagger = \sum_i x_i P_{i,t}^\dagger$ are collective pair operators for neutron-neutron pairs ($t = 1$), proton-proton pairs ($t = -1$) and proton-neutron pairs ($t = 0$).

The isoscalar degrees of freedom are described by the collective isoscalar pair

$$\Delta_0^\dagger = \sum_i y_i D_{i,0}^\dagger. \tag{28}$$

For even-even systems with $N > Z$ the ground state is described by [14]

$$|QCM\rangle = (\tilde{\Gamma}_1^\dagger)^{n_N}(A^\dagger + \Delta_0^{\dagger 2})^{n_q}|0\rangle, \tag{29}$$

where $n_N = (N-Z)/2$ gives the number of neutron pairs in excess. The extra neutrons are represented by the collective neutron pair $\tilde{\Gamma}_1^\dagger = \sum_i z_i P_{i,1}^\dagger$.

The QCM calculations are performed iteratively with the Skyrme-HF calculations. At the convergence, the binding energy is obtained by adding to the mean-field energy the contribution of the pairing energy. The latter is calculated as the average of the pairing force from which it is extracted out the contribution of self-energy terms. For the like-particle pairing these terms are

$$E_{n(p)}^{mf} = \sum_i V^{T=1}(i,i) v_{i,n(p)}^4, \tag{30}$$

while for the pn pairing the expresions are

$$E_{pn}^{mf}(T) = \sum_i V^T(i,i) v_{i,p}^2 v_{i,n}^2. \tag{31}$$

In the present calculations, for the isovector-isoscalar pairing interaction we employ a zero range force of the form:

$$V^T(r_1, r_2) = V_0^T \delta(r_1 - r_2) \hat{P}_{S,S_z}^T \tag{32}$$

where $\hat{P}_{S,S_z}^T$ is the projection operator on the spin of the pairs, namely, $S = 0$ for the isovector force and $S = 1, S_z = 0$ for the isoscalar force. The matrix elements of the pairing interaction (36) for the single-particle states provided by the Skyrme functional are calculated as shown in the Appendix of Ref. [15].

In the Skyrme-HF+QCM calculations for the mean field we consider the Skyrme functional UNE1 [16]. For the strength of the isovector pairing $V_0 = V_0^{T=1}$ and the ratio $w = V_0^{T=0}/V_0^{T=1}$ we have employed various values and finally we have kept the ones for which the differences between the calculated and experimental binding energies are the smallest.

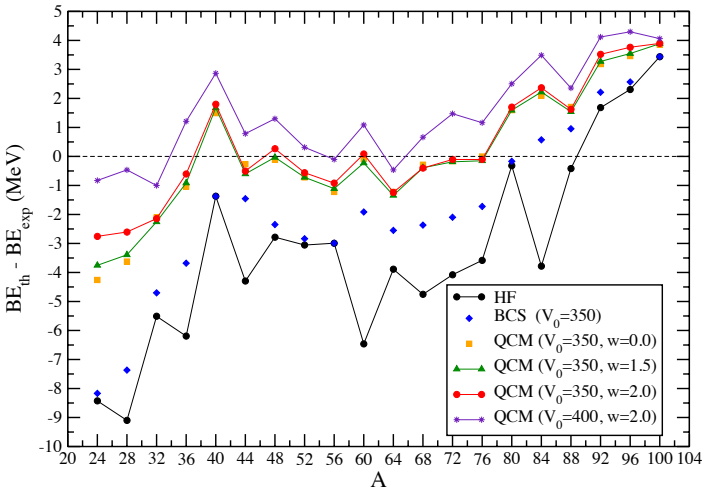

FIG. 7: Binding energies residuals, in MeV, for even-even N=Z nuclei as a function of A=N+Z. The results correspond to the pairing forces indicated in the figure.

A. Pairing and binding energies of $N = Z$ nuclei

The most representative results for the binding energies are presented in Fig. 7. The figure shows the binding energies residuals, i.e., the difference between the theoretical and experimental binding energies. The parameters employed in the calculations are indicated in the figure.

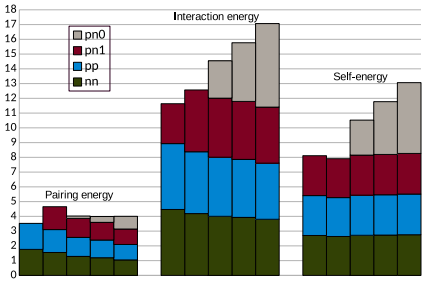

FIG. 8: Pairing energy, interaction energy and self-energy, in MeV, for ^{64}Ge. From the left to the right are shown, for each quantity, the PBCS result and the QCM results for w=$\{0.0, 1.0, 1.5, 2.0\}$. $pn0$ and $pn1$ indicate the T=0 and T=1 pn channels.

From Fig. 7 it can be seen that the binding energies are increasing significantly when

are taken into account the isovector pn pairing correlations, treated in the QCM approach. On the other hand, except for A=24 and A=28, the effect of the isoscalar pn pairing on the binding energies is surprisingly small. This fact is caused by the competition between various pairing channels and between pairing and mean field. As an example, we discuss in detail the results for the nucleus ^{64}Ge, which is illustrating a typical case.

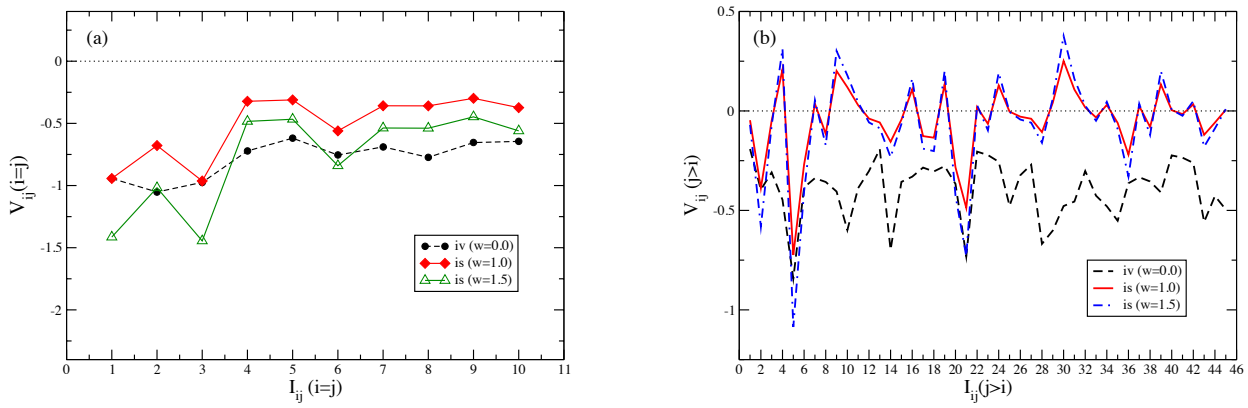

FIG. 9: Diagonal (a) and non-diagonal (b) matrix elements of the isovector and isoscalar pairing force for ^{64}Ge. The quantity I_{ij} enumerates the pair indices of V_{ij}.

In Fig. 8 are shown the pairing energies for ^{64}Ge provided by the QCM calculations for V_0=350 and w=$\{0.0, 1, 1.5, 2\}$. As a reference, in the same figure we have included also the pairing energies provided by the particle-number projected-BCS (PBCS) approach. The PBCS wave function is taken as a product between a neutron and a proton pair condensate, so it does not take into account the isovector pn pairing correlations. The latter are taken into account in the isovector QCM approach (w=0) and, as expected, they increase the total pairing energy compared to PBCS. By contrast, the like-particle pairing energies are larger in PBCS than in QCM. This is due the fact that in isovector QCM the like-particle pairing is competing with the isovector pn pairing because they build up correlations by sharing the same model space. For the same reason, the like-particle and isovector pn pairing energies are decreasing further when the isoscalar pn channel is switched on. Yet, as seen in Fig. 8, in this case the decrease of the isovector pairing is not compensated by the pairing energy gained by opening the isoscalar channel. On the other hand, the contribution of the isoscalar pn channel to the interaction energy is increasing rapidly with the scaling factor w, becoming almost equal to the isovector pn channel for $w = 1.5$. However, as seen from Fig. 8, most of

the interaction energy in the isoscalar channel is coming from the self-energy. As a result, the contribution of the isoscalar pn pairing to the total pairing, in which it is not included the self-energy, is reduced significantly, much more than for the isovector pn pairing. This behavior can be traced back to the matrix elements (m.e.) of the pairing interaction, shown in Fig. 9. Thus, as seen in Fig. 9a, by increasing the scaling factor, some diagonal m.e. of the isoscalar pn pairing become larger than the isovector ones. However, the contribution of diagonal m.e. is drastically reduced when the self-energy terms are subtracted. Therefore, due to the subtraction, the dominant contribution to the pairing energies comes from the off-diagonal m.e., shown in Fig. 9b. It can be noticed that, in average, the m.e. of the isoscalar interaction are smaller than the m.e. of the isovector interaction and, more importantly, some of the isoscalar m.e. are positive. Due to these reasons, the contribution of the isoscalar pairing force to the pairing correlations is not increasing significantly with the scaling factor. In addition, in self-consistent Skyrme-HF+QCM calculations, the variation of the pairing energies can be compensated by the mean field energy. In this case, when the isoscalar channel is turned on, the mean field energy is increasing by about 530 keV for w=1.5 and by 540 keV for w=2.0, while the total pairing energy is decreasing, relative to the isovector pairing, by about the same quantity. As a consequence, as seen in Fig. 7, the total binding energy of ^{64}Ge is not changing much when the isoscalar pairing force is turned on.

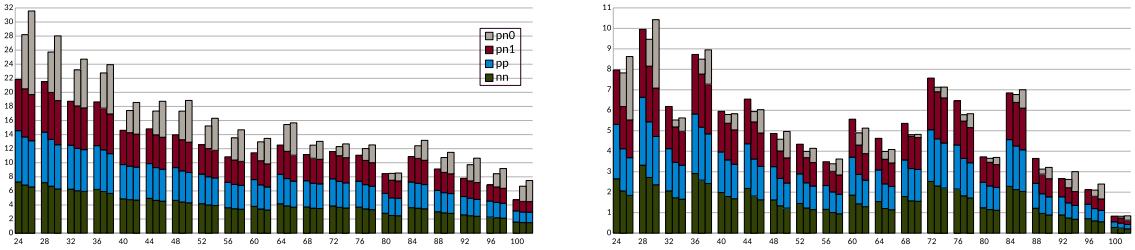

FIG. 10: Interaction energies (left) and pairing energies (right), in MeV, for $N = Z$ nuclei. For each nucleus are shown, from the left to the right, the results for w=$\{0.0, 1.5.2.0\}$

The pairing energies and the interaction energies provided by the self-consistent calculations for all $N = Z$ nuclei are shown in Fig. 10. It can be seen that in the majority of nuclei these quantities have a similar pattern as in the example discussed above.

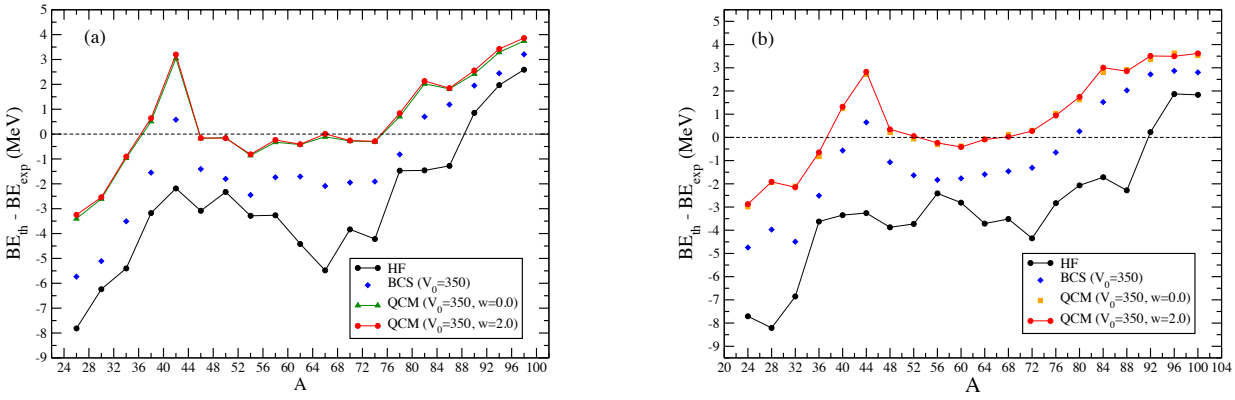

FIG. 11: The residuals, function of $A = N + Z$, for $N = Z + 2$ (a) and $N = Z + 4$ (b) nuclei.

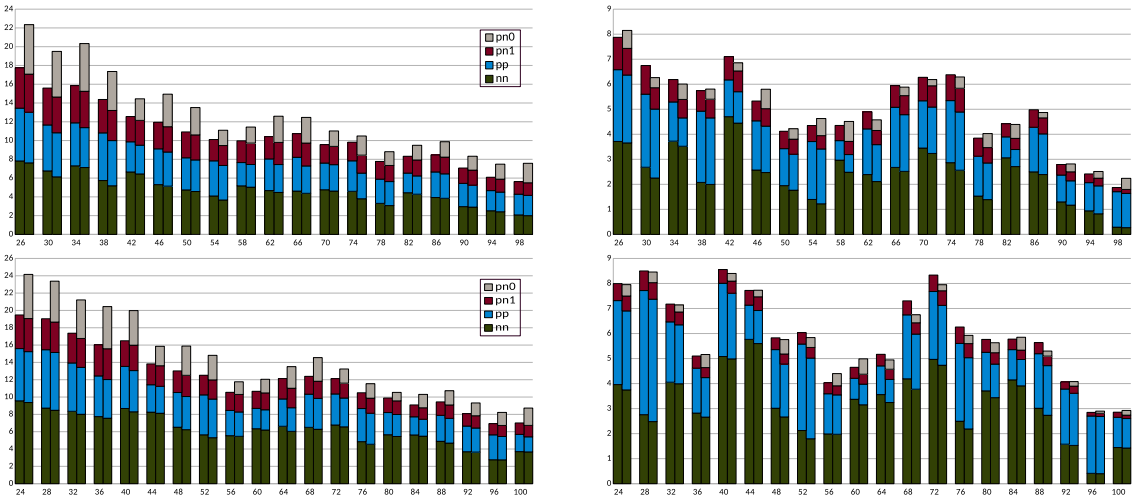

FIG. 12: Interaction energies (left) and pairing energies (right), in MeV, function of $A = N + Z$, for the nuclei with $N = Z + 2$ (top) and $N = Z + 4$ (bottom). For each nucleus are shown, from the left to the right, the results for w= $\{0.0, 2.0\}$

B. Pairing and binding energies of $N > Z$ nuclei

To study how the pairing correlations are affected by the extra neutrons added to N=Z nuclei, we take as examples the nuclei with $N = Z + 2$ and $N = Z + 4$ and with atomic mass $20 < Z < 100$. The binding energy residuals for these nuclei are given in Fig. 11. Are shown the results for the pairing force with V_0=350 and $w = \{0.0, 2.0\}$. The contribution of the pairing energies to the binding energies is displayed in Fig. 12. For reference, in Fig. 12 are given also the interaction energies. The latter are increasing significantly when

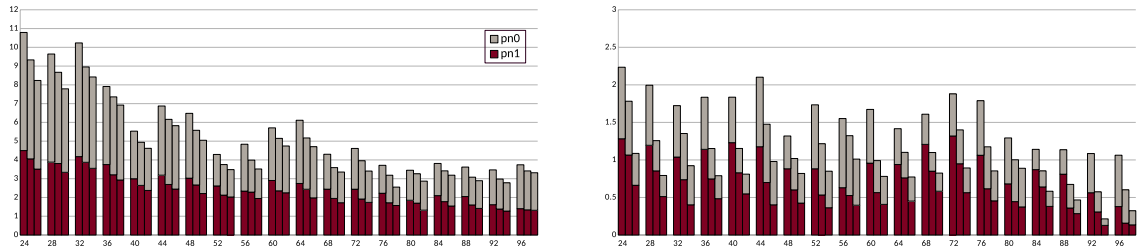

FIG. 13: Interaction energies (left) and pairing energies (right) for T=0 and T=1 pn pairing and for $w = 2.0$. The results, from the left to the right, are for the nuclei with $N = Z$, $N = Z + 2$ and $N = Z + 4$. On x-axis is indicated the atomic mass of $N = Z$ nuclei.

the isoscalar pairing is turned on. On the contrary, this is not the case for the pairing energies. However, this does not mean, however, that the isoscalar pairing correlations do not contribute to the binding energy of $N > Z$ nuclei. This can be seen clearly from Fig. 13, which shows how the pn pairing energies and interaction energies are changing by adding neutrons to the $N = Z$ nuclei. In both T=0 and T=1 channels these energies are decreasing when more neutrons are added. However, they are not vanishing, including for the nuclei with $N = Z + 4$, and they coexist in all the nuclei. In fact, this is happening not only for the large isoscalar strength considered here, but also for any QCM calculations with an isovector-isoscalar pairing force with $w > 0$.

Summarizing, we have discussed the contribution of isovector and isoscalar pairing on binding energies of $N = Z$ nuclei and of $N > Z$ nuclei with $N = Z + 2$ and $N = Z + 4$. An interesting aspect pointed out by these calculations is the strong interdependence between all types of pairing correlations. In particular, when the isoscalar pn pairing channel is switched on, the pairing correlations are redistributed among all the pairing channels without changing significantly the total pairing energy. Due to this reason, for the majority of $N \approx Z$ nuclei the binding energy is not affected much when the isoscalar pairing channel is switched on. Yet, in all the calculations which include both the isovector and the isoscalar pairing forces, the isoscalar pairing correlations contribute significantly to the binding energies and coexist always with the isovector pn pairing. This feature is related to the exact conservation of the particle number and the isospin by the QCM approach.

[1] M. Sambataro and N. Sandulescu, Phys. Lett. B **820**, 136476 (2021)

[2] M. Sambataro and N. Sandulescu, arXiv:2112.04370, submitted to Phys. Lett. B

[3] D. Negrea, N. Sandulescu, D. Gambacurta, arXiv:2111.00878, submitted to Phys. Rev. C

[4] N. Sandulescu, D. Negrea, J, Dukelsky, C.W. Johnson, Phys. Rev. C **85**, 061303(R) (2012).

[5] N.Sandulescu, D. Negrea, D. Gambacurta, Phys.Lett. B **751**, 348 (2015).

[6] M. Sambataro and N. Sandulescu, Phys. Rev. C **88**, 061303(R) (2013).

[7] M. Sambataro and N. Sandulescu, Phys. Rev. C **93**, 054320 (2016).

[8] B.A. Brown, W.A. Richter, Phys. Rev. C 74, 034315 (2006).

[9] B. F. Bayman, Nucl. Phys. 15, 33 (1960).

[10] M. Blatt, Prog. Theor. Phys. (Kyoto) 24, 851 (1960).

[11] I. Talmi, Nucl. Phys. A172, 1 (1971).

[12] A. Poves and G. Martinez-Pinedo, Phys. Lett B **430**, 203 (1998).

[13] R. Sheline, S. Kubono, K. Morita, and M. Tanaka, Phys. Lett. B **119**, 263 (1982).

[14] N. Negrea, P. Buganu, D. Gambacurta, N. Sandulescu, Phys. Rev. C **98**, 064319 (2018).

[15] D. Gambacurta, D. Lacroix, Phys. Rev. C **91**, 014308 (2015).

[16] K. Kortelainen et al, Phys. Rev.C **85**, 024304 (2012).

[17] A. Volya, V. Zelevinsky, Phys. Lett. B **574**, 27 (2003).

[18] F. Simkovic, C. Moustakidis, L. Pacearescu, A. Faessler, Phys. Rev. C **68**, 054319 (2003).

Project coordinator

Dr. N. Sandulescu